



Received on 17 January, 2017; received in revised form, 31 March, 2017; accepted, 27 May, 2017; published 01 August, 2017

## DESIGN AND SYNTHESIS OF BI-METALLIC PORPHYRIN ARRAY

S. Tamijselvy <sup>\*1</sup> and R. Venkatesan <sup>2</sup>

Department of Chemistry <sup>1</sup>, Vels University, Chennai, Tamil Nadu - 600117, India.

Department of Chemistry <sup>2</sup>, Pondicherry University, R.V. Nagar, Kalapet, Pondicherry - 605014, India.

### Keywords:

Porphyrin, Monocuperated,  
Physico-chemical, Electron  
Paramagnetic Resonance (EPR)

### Correspondence to Author:

**Dr. S. Tamijselvy**

Assistant Professor,  
School of Basic Sciences,  
Department of Chemistry,  
Vels University, Chennai,  
Tamil Nadu - 600117, India.


**E-mail:** tamijselvy@gmail.com

**ABSTRACT:** Porphyrins are ever-present large class of naturally occurring macrocyclic compounds with many significant biological representatives comprising heme and chlorophyll. Novel bi-metallic porphyrins derived from [5-(4-hydroxyphenyl)-10,15,20-tri(4-methyl phenyl) porphyrin] and salicylideneamino-2-(N,N-dimethylamino) ethane copper (II) perchlorate was obtained in good yields. The results from various physico-chemical studies reveal a change in the geometry of the copper environment after coordination at the periphery of the porphyrin. The EPR of monocuperated metalloporphyrins have signals of copper with planar geometry and lacks the lines corresponding to peripheral metal due to dipolar broadening. Weak interaction between the metal centers is clear from nickel porphyrin.

**INTRODUCTION:** Design and synthesis of porphyrins with array of oligomers or metals substituted analogs having well-defined shapes and sizes are currently of great interesting topics to modify the photophysical properties, absorption cross-section, catalytic reactions and energy transfer reactions <sup>1-3</sup>. In recent years, peripheral substitution, mostly at *meso*-positions, of platinum group metal ions has been employed in synthesizing dimeric and oligomeric type porphyrins that undergo interesting intramolecular photo processes between the porphyrin sub-units <sup>4-7</sup>. Most examples deal with porphyrins bearing *meso*-pyridyl groups, since the wide coordination possibility of pyridine group allows large assemblies to be built <sup>8</sup>.

Even though the existing peripherally metal substituted porphyrins help to understand the interaction between porphyrin rings, such systems are not suitable to study the interaction between the metal centers. Monomeric porphyrin systems with peripherally coordinated metal ions would be an ideal choice for such studies. An example in this kind of porphyrins is bimetallic (nickel/palladium) porphyrin monomer has been synthesized <sup>7</sup>. However, till date, no study has been conducted with magnetically active paramagnetic metal ions substituted around a porphyrin ring forming *meso*-monometallated porphyrin monomers.

The coordination of paramagnetic metal ion offers great advantage in probing the interaction between the metal ions. Regarding the coordination of paramagnetic metal ion at the peripheral positions of the porphyrin, an earlier report suggests that the coordination of copper (II) at the 8-hydroxyquinoline position of 5,10,15,20-tetrakis(8-hydroxyquinolyl) porphyrin occurs faster than at the central porphyrin core <sup>9</sup>.

<b>QUICK RESPONSE CODE</b> 	<b>DOI:</b> 10.13040/IJPSR.0975-8232.8(8).3361-70
	Article can be accessed online on: <a href="http://www.ijpsr.com">www.ijpsr.com</a>
<b>DOI link:</b> <a href="http://dx.doi.org/10.13040/IJPSR.0975-8232.8(8).3361-70">http://dx.doi.org/10.13040/IJPSR.0975-8232.8(8).3361-70</a>	

The application of such multi metal complexes could probably lie in synthesizing better catalysts and energy storage systems<sup>10</sup>.

Here, we report the synthesis of a neutral bi-metallic complex with *meso*-5-(4-hydroxyphenyl)-10,15,20-tris(4-methylphenyl)porphyrin as the base porphyrin. From the literature survey, we believe that this is the first report of this type of compound. Here in, we report the synthesis, characterization and electron spin resonance spectral study of mono cuperated porphyrins derived from [5-(4-hydroxyphenyl) - 10, 15, 20 - tri (4-methylphenyl) porphyrinato]copper, [5-(4-hydroxyphenyl)-10,15, 20-tri(4-methylphenyl) porphyrinato]vanadyl, [5-(4-hydroxyphenyl)- 10, 15, 20- tri(4-methylphenyl) porphyrinato] nickel.

**MATERIALS AND METHODS:** 4-methoxy benzaldehyde, pyrrole and propionic acid were bought from SD fine, India, were used after purification<sup>11</sup>. All the solvents used were analytical grade and were dried further whenever required. <sup>1</sup>H-nmr spectra of free porphyrins were recorded on AMX-400 NMR spectrometer in CDCl<sub>3</sub>/DMSO, using TMS as the internal standard. FAB mass spectra were recorded on a JEOL SX 102/DA-6000 mass spectrometer/Data system using Argon/Xenon (6 kV, 10mA) as the FAB gas. Electronic absorption spectra were obtained with Ocean optics optical fiber (400 μm) spectrophotometer SD1000 using 10 mm quartz cell. X-band EPR spectra were recorded with JEOL JES-TEs 100 ESR spectrometer having 100 kHz field modulation. Spectra at liquid nitrogen temperature were performed in a cold finger Dewar. IR spectra were recorded on ABB Bomem MB 104 spectrometer using KBr disks. Elemental (C, H and N) analysis was performed with Heraeus Rapid analyzer.

All electrochemical experiments were performed using Ecochemie AUTOLAB PGSTAT 12 controlled by GPES software running under Microsoft Windows. A conventional three-electrode setup was employed in all electrochemical measurements, with tetrabutyl ammonium perchlorate as supporting electrolyte. Generally all the cyclic voltammogram were performed with scan rate of 50mV/s.

For recording square wave voltammogram a constant frequency of 8 Hz with step potential of 4mV and pulse amplitude of 10 mV was employed.

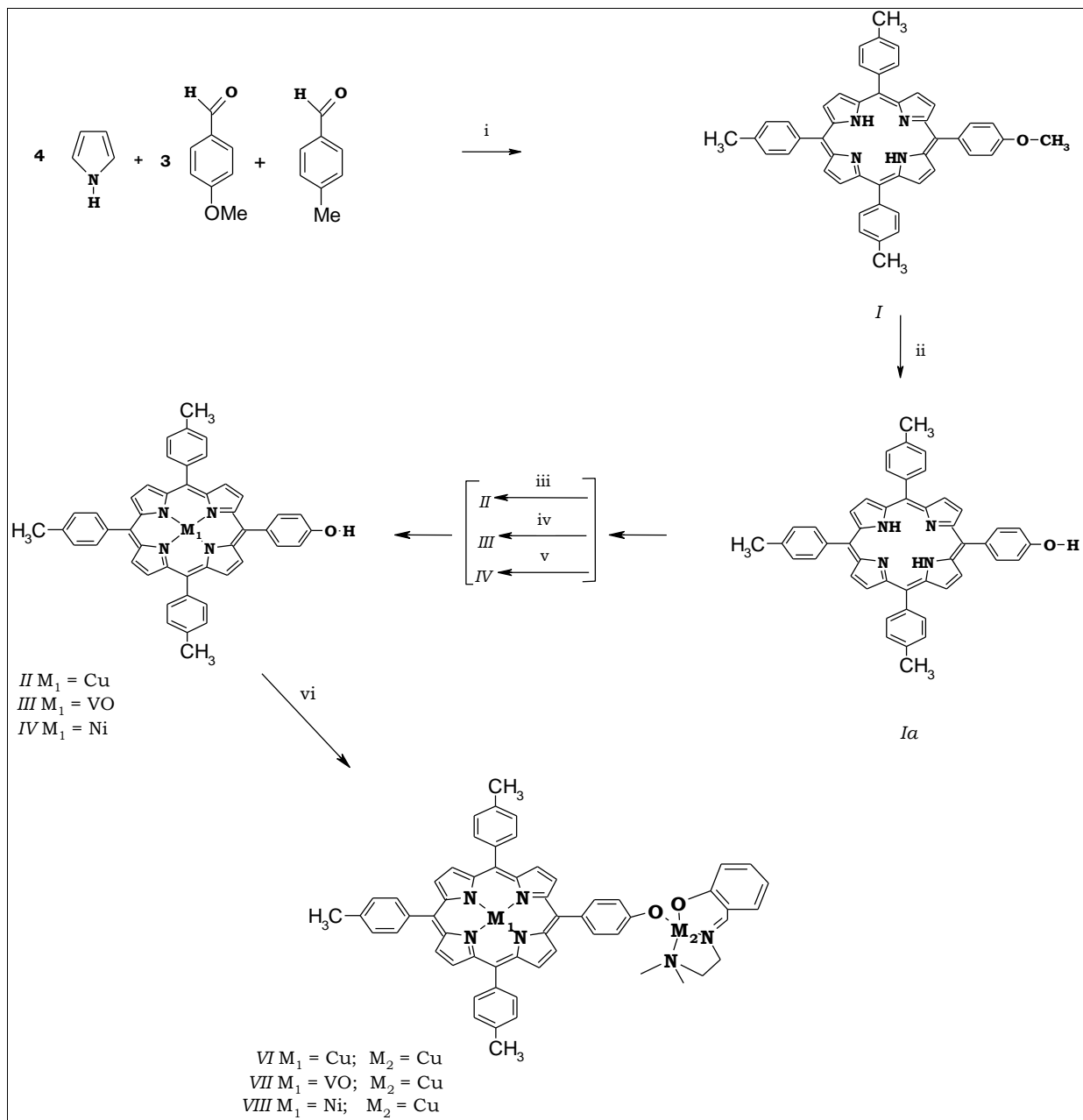
**Experimentals Section:** The precursor ligands, *Meso*-5-(4-methoxyphenyl)-10,15,20-tris(4-methylphenyl)porphyrin<sup>12</sup> (*I*), *Meso*-5-(4-hydroxyphenyl)-10,15,20-tris (4-methylphenyl) porphyrin<sup>13</sup> (*Ia*), *Meso*-[5-(4-hydroxyphenyl)-10,15,20-tri(4-methylphenyl)porphyrinato] copper(II) (*II*)<sup>14</sup>, *Meso*-[5-(4-hydroxyphenyl) - 10, 15, 20- tri (4-methylphenyl) porphyrinato] vanadyl(II) (*III*)<sup>14</sup>, *Meso*-[5-(4-hydroxyphenyl) - 10, 15, 20-tri (4-methylphenyl) porphyrinato] nickel(II) (*IV*)<sup>14</sup>, Salicylideneamino-2- (N,N-dimethylamino) ethane (*L*)<sup>15</sup>, Salicylidene amino-2-(N,N-dimethylamino) ethane copper (II) perchlorate monohydrate, CuLClO<sub>4</sub>.H<sub>2</sub>O, (*V*)<sup>15</sup> were synthesized from the earlier procedures. <sup>1</sup>H NMR was used to confirm the purity of the free base porphyrins.

**Scheme of Synthesis:** The synthesis of *meso*-monocuperated metalloporphyrins are achieved by two-step procedure. Firstly, the required metalloporphyrins were prepared and further reaction with the tri-coordinated Schiff's based copper complex, CuLClO<sub>4</sub>, results in coordination of copper Schiff's base at the *para* position of *meso*-4-hydroxyphenyl group (**Scheme I**). This methodology has afforded us to prepare both homo and hetero metallic molecular systems. In the absence of single crystal structure, **Scheme I** shows a speculative molecular structure. Compounds *VI*, *VII* and *VIII* are stable in air.

***Meso*-[5-((4-hydroxosalicylideneamino-2- (N, N-dimethylamino) ethanecopper(II)) phenoxo)-10, 15,20-tri(4-methylphenyl)porphyrinato] copper (II) (VI):** To 75 mL of nitrogen bubbled dry dimethylformamide, *II* (0.5 mmole, 0.49 g) was added. 0.1 mmoles (0.02 g) of anhydrous potassium carbonate was added and purging of nitrogen was continued for further 1 hour. The reaction mixture was then refluxed for 24 hours under nitrogen atmosphere. 0.6 mmoles (0.213 g) of *V* was then added and purging was continued for another 30 minutes, followed by refluxion under nitrogen atmosphere for another 24 hours. The volume of the resultant solution was reduced to one fourth under vacuum and then extracted with

dichloromethane. The organic layer was washed with water, dried over anhydrous sodium sulfate and concentrated under reduced pressure. Pure VI was obtained by column chromatography on basic alumina using hexane and chloroform as eluant in the ratio of 4:6. The  $R_f$  value on an alumina-coated

plate was found to be 0.5 in the above-mentioned mixture of solvent. Yield 0.099 g (20%). IR (KBr): 3423, 2921, 2853 and 1649  $\text{cm}^{-1}$ ; FAB-MS,  $m/z$ : calculated for  $\text{C}_{60}\text{H}_{50}\text{O}_3\text{N}_6\text{Cu}_2\text{Cl}_2$ : 1099; found: 1099,  $[\text{M}]^+$ .



**SCHEME I:** (i)  $\text{CH}_3\text{CH}_2\text{COOH}$ , REFLUX, 30MIN; (ii) PYRIDINE HYDROCHLORIDE, REFLUX, 130°C, 4H; (iii)  $\text{Cu}(\text{OAc})_2$ , DMF, HEAT, 30MIN; (iv)  $\text{VO}(\text{acac})_2$ , PHENOL, REFLUX, 3h; (v)  $\text{NiCl}_2$ , DMF, HEAT, 30MIN; (vi)  $(\text{CuL})\text{ClO}_4$ , DMF/ $\text{K}_2\text{CO}_3$ ,  $\text{N}_2$  ATMOSPHERE, 24H, REFLUX

Note: Hydrogen and coordinated solvent molecules are not shown for clarity

**Meso-[5-((4-hydroxosalicylideneamino-2-(N, N-dimethylamino)ethanecopper(II) phenoxo) - 10, 15, 20-tri (4-methylphenyl) porphyrinato) vanadyl (II) (VII):** Compound VII was synthesized using a similar procedure described for VI except

that III (0.5 g, 0.7 mmol) was used instead of II. Pure VII was obtained by column chromatography on basic alumina using hexane and chloroform as eluant in the ratio of 4:6. The  $R_f$  value on an alumina-coated plate was found to be 0.5. Yield

0.069 g (10%). IR (KBr): 3425, 2925, 2853 and 1652  $\text{cm}^{-1}$ .

**Meso-[5-((4-hydroxosalicylideneamino-2-(N, N-dimethylamino) ethanecopper(II)) phenoxo) -10, 15,20-tri(4-methylphenyl)porphyrinato] nickel (II)(VIII):** Compound VIII was prepared by adapting a parallel procedure described for VI except that IV (0.5 g, 0.7 mmol) was used instead of II. Pure VIII was obtained by column chromatography on basic alumina using hexane and chloroform as eluant in the ratio of 4:6. The  $R_f$  value on an alumina-coated plate was found to be 0.5. Yield 0.14 g (20%). IR (KBr): 3436, 2925, 2853 and 1650  $\text{cm}^{-1}$ ; FAB-MS, m/z: calculated for  $\text{C}_{62}\text{H}_{61}\text{N}_6\text{O}_6\text{CuNiCl}_2$ : 1249; found: 1249,  $[\text{M}]^+$ .

## RESULTS AND DISCUSSION:

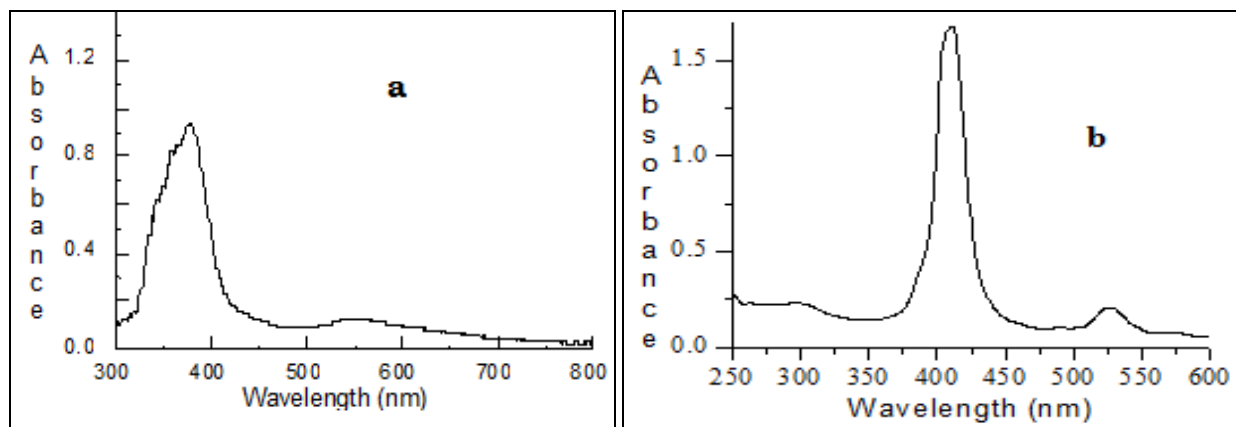
**UV-Visible studies:** The electronic absorption spectra of II, III and IV reveal transitions in the expected lines<sup>2</sup>. On coordination with V at the

peripheral site, the Soret band maximum of VI, VII and VIII showed a red shift with respect to metalloporphyrins. Similarly, the Q band absorption energy was also found to shift slightly towards lower energy with increased broadness, which is due to meso-position perturbation of the porphyrin ring.<sup>16</sup> The coordination of copper at the periphery in the complexes VI, VII and VIII was clearly depicted by the increased intensity in the region greater than 550 nm which arises due to the overlap of ligand field transition of copper in CuL units with the strong Q band of metalloporphyrins. Since, the electronic transitions of the individual units in VI, VII and VIII neither showed any major change nor new transitions were observed, it was clear that the electronic interactions between porphyrin ring and CuL units were negligible. The electronic absorption data are given Table 1 and the spectrum is given in Fig. 1.

**TABLE 1: ELECTRONIC ABSORPTION MAXIMUM AND VOTAMMETRIC DATA OF VARIOUS MESO-SUBSTITUTED PORPHYRINS (0.1mM)**

S. No.	Complex	Absorption maximum (nm)	Oxidation Potential <sup>a</sup> in V			Reduction Potential <sup>a</sup> in V		
			$\text{P} \rightleftharpoons \text{P}^+$	$\text{P}^+ \rightleftharpoons \text{P}^{2+}$	$\text{Cu}^{2+} \rightarrow \text{Cu}^{3+}$	$\text{Cu}^{2+} \rightarrow \text{Cu}^+$	$\text{P} \rightleftharpoons \text{P}^-$	$\text{P}^- \rightleftharpoons \text{P}^{2-}$
1.	I	411, 505, 539, 578, 635	0.972	1.224	---	---	-1.266	-1.628
2.	Ia	409, 502, 535, 572, 631	0.743	1.178	---	---	-1.260	-1.680
3.	II	407, 525	0.9	1.261	---	---	-1.429	-1.879
4.	III	414, 530	0.849	1.170	---	---	-1.486	---
5.	IV	408, 514	0.986	1.216	---	---	-1.393	-1.966
6.	V	353, 377, 554	---	---	1.229	-0.472	---	---
7.	VI	411, 527, 571, 305	0.920	1.173	1.373	-0.489	-1.073	-1.411
8.	VII	408, 515, 322	0.667	0.989	1.48	-0.659	-1.104	-1.393
9.	VIII	413, 529, 572, 268	0.673	0.945	1.270	-0.558	-0.618	-1.274

\*P = Porphyrin; a: redox potentials are measured with 1mM TBAP as supporting electrolyte in a three electrode system with 2mm pt disc as working electrode. All potentials are with respect to SCE (0.24 V)



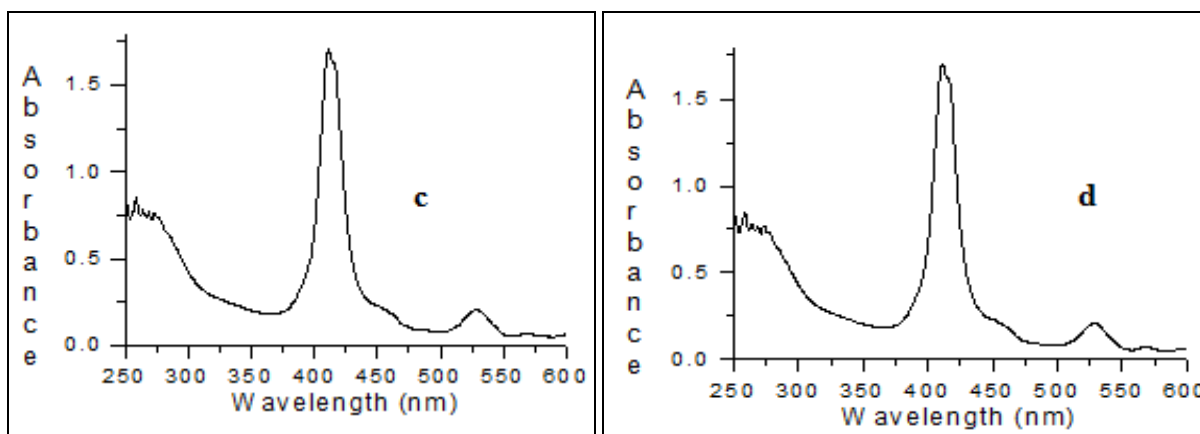


FIG. 1: ELECTRONIC ABSORPTION SPECTRUM IN 10mm PATHLENGTH (0.01mm) DICHLOROMETHANE SOLUTION OF (a) V (b) VI (c) VII AND (d) VIII

**Voltammetric studies:** The electrochemical properties of VI - VIII can be explained in terms of the contribution from all the constituents by which it was made up of. The electrochemical behaviour of II to IV were clearly understood from the voltammogram, (see Fig. 2), it represents two step

one electron reversible oxidation and two step one electron reduction<sup>16,17</sup>. The redox processes can be summarized as

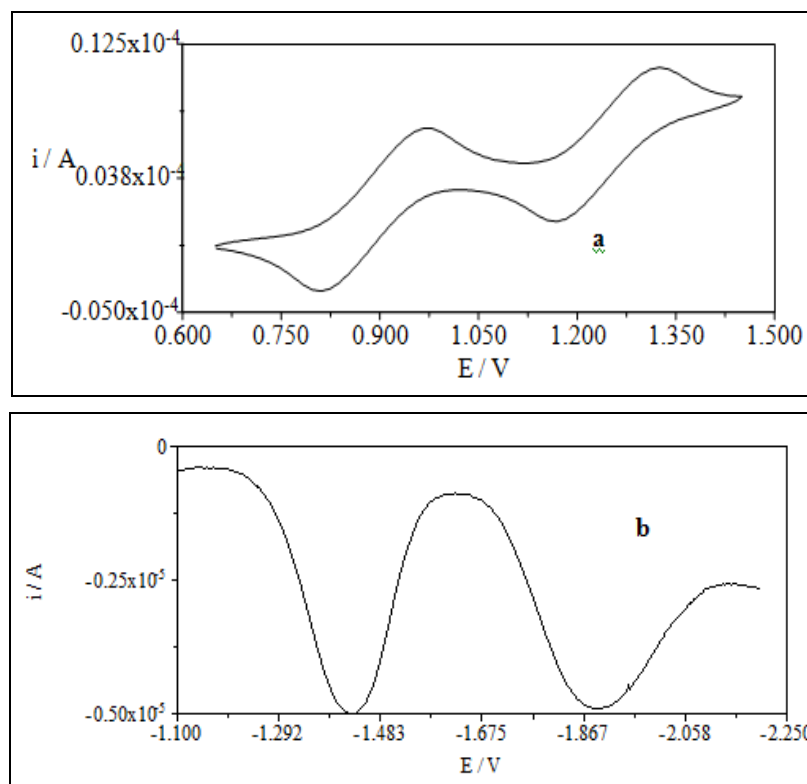
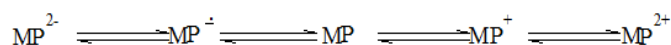


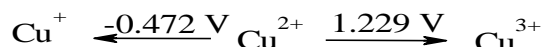
FIG. 2: CYCLIC VOLTAMMOGRAM REPRESENTING OXIDATION OF II (0.1 mM) AT THE SCAN RATE OF 50mV, IN ACETONITRILE (a) AND SQUAREWAVE VOLTAMMOGRAM REPRESENTING REDUCTION OF II (0.1 mM) IN DICHLOROMETHANE (b) WITH 1mM TBAP AS SUPPORTING ELECTROLYTE AND SCE AS THE REFERENCE ELECTRODE

The cyclic voltammogram of metal precursor V in acetonitrile (Fig. 3) results in single oxidation process in the potential range of 0 to 1.5 V and peak at 1.229 V was attributed to the oxidation

couple arising due to oxidation of copper(II) to copper(III). Similarly, in the range of 0 to -1.5 V the compound V shows an irreversible reduction processes at -0.472 V and the reverse scan shows



an anodic peak at -0.2 V which is due to reoxidation of copper (0) to copper (II). It is well known that copper (I) to copper (0) occurs at -0.8 V in acetonitrile<sup>18</sup>. Furthermore, the copper (II) to copper (I) is irreversible due to large geometrical change involved during the process of reduction<sup>19</sup>. The electrochemical processes occurring can be summarized as



The electrochemical behaviour of the complexes VI, VII and VIII can be explained in terms of the contribution from all the constituents by whom it

was made up of. Thus in the range of 0.5 to 1.5 V shows three oxidation peaks, of which the first two oxidation peaks at around 0.6 to 0.9 V and at around 0.95 to 1.0 V were assigned to the oxidation of porphyrin while that around 1.4 V is assigned to the oxidation of copper at the periphery. Various kinetic criterions were employed to understand the nature of the charge transfer process and were summarized as below

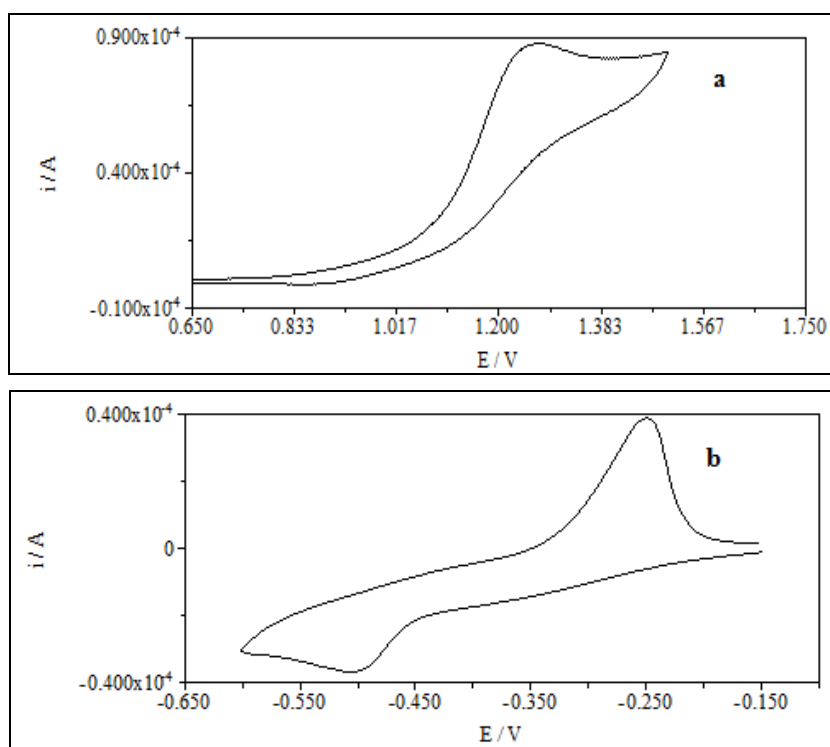
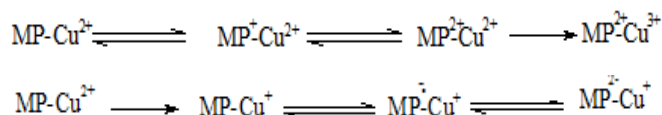


**FIG. 3: CYCLIC VOLTAMMOGRAM REPRESENTING THE OXIDATION (A) AND REDUCTION (B) OF V (0.1 mM) AT THE SCAN RATE OF 50mV, IN METHANOL WITH 1mM TBAP AS SUPPORTING ELECTROLYTE AND SCE AS THE REFERENCE ELECTRODE**

The peak height of the first two redox couples, (arising due to porphyrin oxidation), were found to be equal to the third peak, ( $\text{Cu}^{3+/2+}$ ) which was an indicative of the number of metal precursor present in the complexes. The peak potential ( $E^\circ = 1.4 \text{ V}$ , say in VII) corresponding to the peripheral copper redox process was found to be more positive than in the precursor V ( $E^\circ = 1.2 \text{ V}$ ). This shift was taken as a bench marking for the formation of the copper complex. Any unreacted copper precursor complex, V, would have shown oxidation at 1.2 V instead of 1.4 V. This was also confirmed by

intentional addition of one equivalents of V to either II, III etc. The electrochemical behaviour of impurity added samples behaved in a way, in which the resultant voltammogram can be interpreted as superposition of two individual components. The redox potentials were tabulated in the **Table 1**. The more positive oxidation potential of copper in the complexes indicates the difficulty of it to undergo oxidation. This discrepancy in the oxidation potential arises probably due to shift in the electron density towards phenoxo group.

The depletion in the electron density in the porphyrin core was also clear from the easiness with which it undergoes reduction. The electrochemical study of the complexes (see **Fig. 4**) in the range of  $-0.3$  to  $-1.5$  V, result in three cathodic processes. The peak at  $-0.4$  to  $-0.6$  V was assigned to the reduction process taking place in the peripheral copper ion and the other two potentials were assigned to the reduction processes taking place at the porphyrin  $\pi$  cloud. It was clear from the redox potentials, the oxidation and reduction of the copper(II) at the porphyrin periphery was difficult in *VI*, *VII* and *VIII* in comparison with that of the precursor *V*.

Since on coordination of *V* to the periphery of any metalloporphyrin resulting in a planar geometry hence the oxidation and reduction processes becomes difficult than in *V*. On the other hand, the oxidation and reduction of porphyrin ring seems to be easier in the complexes than the corresponding precursor was possibly due to increased distortion of the porphyrin ring on periphery coordination.

**EPR studies:** The EPR spectra of polycrystalline powder of all the metalloporphyrins at room temperature showed featureless broad lines. Similarly, the solution spectrum in ethanol or dichloromethane at room temperature showed isotropic  $g$  and  $A$  values. As expected the EPR spectra at 77K exhibited an anisotropic EPR spectra typical of copper(II) centers with well determined hyperfine lines arising due to interaction between delocalized  $\pi$  electrons and the nuclear spin  $I_{Cu}=3/2$ . The value obtained by simulated spectra was given in **Table 2**.

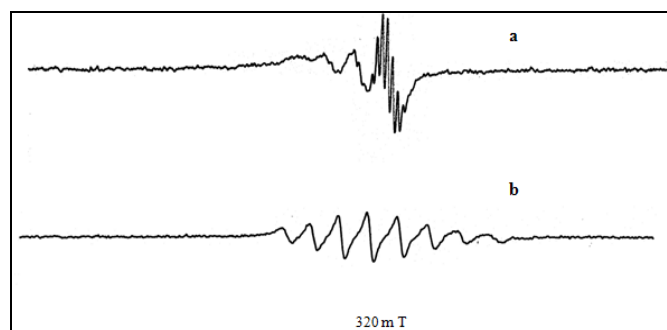


**FIG. 5: ROOM TEMPERATURE EPR SPECTRUM OF VI (a) AND VII (b) IN THE RANGE OF 320**

**TABLE 2: EPR SPIN HAMILTONIAN PARAMETERS OF VARIOUS MESO-SUBSTITUTED PORPHYRINS AT 77K**

S. No.	Compound	$g_{\parallel}$	$g_{\perp}$	$A_{\parallel}^*$	$A_{\perp}^*$	$A_{\parallel}^{N*}$	$A_{\perp}^{N*}$	$g_{iso}$	$A_{iso}^*$	$f^{db}$
1.	<i>II</i>	2.190	2.045	196.3	34	19.8	14.2	2.093	88.77	111.56
2.	<i>III</i>	1.965	1.982	169.2	56.4	2.9	2.8	1.976	94.0	116.13
3.	<i>V</i>	2.260	2.072	185	16.8	13	13	2.135	72.87	122.16
4.	<i>VI</i>	2.198	2.055	195.9	32	18	13.6	2.103	86.63	112.20
		2.222	2.067	186	17	12.5	11	2.119	73.33	119.46
5.	<i>VII</i>	1.962	1.982	168.9	56.5	2.9	2.8	1.975	93.97	116.16
		2.205	2.053	185	16.8	13	13	2.104	72.87	121.15
6.	<i>VIII</i>	2.226	2.065	180	17.8	10.3	10.3	2.119	71.87	123.67

\*Coupling constants are in  $cm^{-1}$  and multiplied by  $10^4$ , <sup>b</sup> the parameter  $f$  is given by  $g_{\parallel}/A_{\parallel}$

The EPR spectrum of precursor *V* at 77K, (**Fig. 6**), shows four line pattern and spin Hamiltonian parameters are estimated through simulation as  $g_{\parallel}=2.260$ ,  $A_{\parallel}^{Cu}=18.5$  mT,  $A_{\parallel}^N=1.30$  mT,  $g_{\perp}=2.072$ ,  $A_{\perp}^{Cu}=1.68$  mT,  $A_{\perp}^N=1.30$  mT. The observed  $g$  and  $A$  values suggest that the copper exists in a more distorted geometry <sup>20</sup>. This geometrical distortion arises due to the flexibility of the Schiff's ligand.

The ethanolic frozen solution EPR spectrum of *II* (**Fig. 7**) shows a typical axially symmetric Cu (II) ion spectrum coordinated at the center of the porphyrin core. The unpaired electron in  $d_{x^2-y^2}$  orbital of copper (II) ion, with electronic ground

state  $^2B_1$ , gives rise to two sets of metal hyperfine lines corresponding to  $g_{\parallel}$  and  $g_{\perp}$  values. The first two components of the four copper hyperfine lines in the parallel region are well resolved in low field and the third component is slightly merged with the much stronger perpendicular line to the different extent while the fourth parallel line is completely overlapped.

The appearance of super hyperfine lines from four nitrogen atom indicates the coordination of copper at the center of the porphyrin core. The simulation of EPR spectrum allowed us to estimate accurately, the spin Hamiltonian parameters as  $g_{\parallel}=2.190$ ,  $A_{\parallel}^{Cu}=19.63$  mT,  $A_{\parallel}^N=1.98$  mT,  $g_{\perp}=2.045$ ,  $A_{\perp}^{Cu}=3.4$

mT,  $A_{\perp}^N=1.42$  mT and the values are summarized in **Table 2**. The observed trend is in conformity with earlier results<sup>21</sup>.

The spectrum of *III* clearly shows two sets of eight vanadyl ( $I = 7/2$ ) hyperfine splitting pattern and further simulation (**Fig. 8**) confirms the assignment and the spin Hamiltonian values are given in **Table 2**, which matches with earlier observed values<sup>21</sup>.

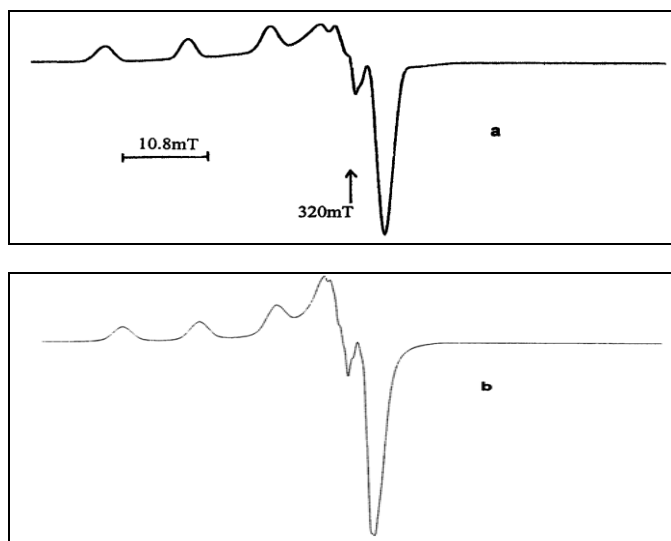


**FIG. 6:** ESR SPECTRUM OF *V* IN ETHANOL AT 77 K. (a) EXPERIMENTAL; (b) SIMULATED. THE SIMULATED PARAMETERS ARE  $g_{\parallel}=2.260$ ,  $g_{\perp}=2.072$ ,  $A_{\parallel}^{Cu}=18.5$  mT,  $A_{\perp}^{Cu}=1.68$  mT,  $A_{\parallel}^N=1.3$  mT,  $A_{\perp}^N=1.3$  mT. LINE WIDTH: PARALLEL = 1.6 mT, PERPENDICULAR = 1.6 mT.  $\nu = 9.053$  GHz

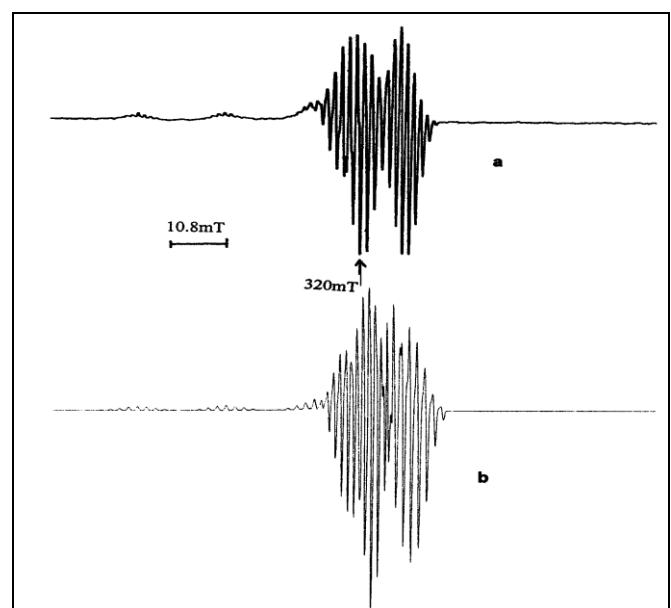


**FIG. 7:** ESR SPECTRUM OF *II* IN ETHANOL AT 77 K. (a) EXPERIMENTAL; (b) SIMULATED. THE SIMULATION PARAMETERS ARE  $g_{\parallel}= 2.19$ ,  $g_{\perp}=2.045$ ,  $A_{\parallel}^{Cu}=19.6$  mT,  $A_{\perp}^{Cu}=3.4$  mT,  $A_{\parallel}^N=1.98$  mT,  $A_{\perp}^N=1.42$  mT. LINE WIDTH: PARALLEL = 0.55 mT, PERPENDICULAR = 0.4 mT.  $\nu = 9.062$  GHz

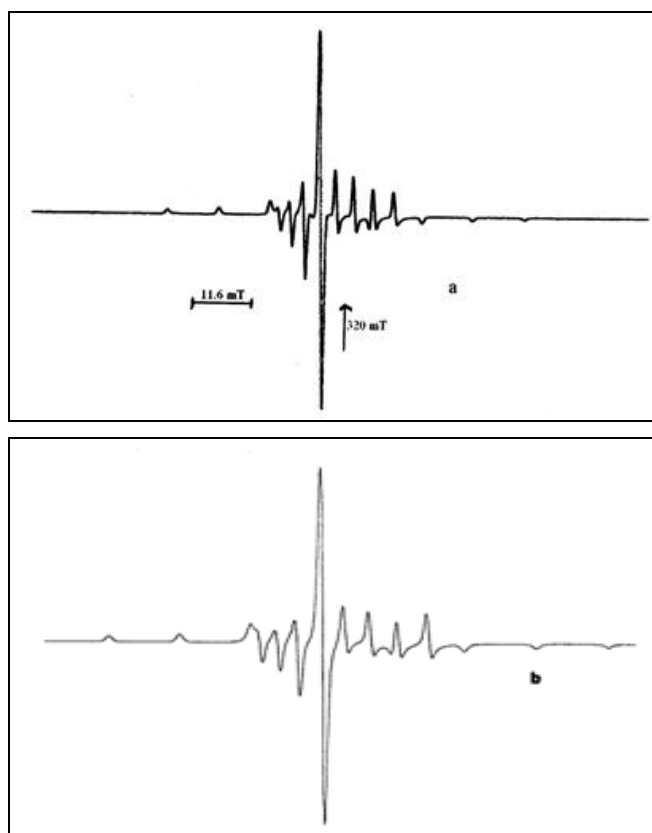


**FIG. 8:** EPR SPECTRUM OF *III* IN ETHANOL SOLUTION AT 77 K. (a) EXPERIMENTAL; (b) SIMULATED. THE SIMULATION PARAMETERS ARE  $g_{\parallel}=1.965$ ,  $g_{\perp}=1.982$ ,  $A_{\parallel}^V=16.9$  mT,  $A_{\perp}^V=5.64$  mT,  $A_{\parallel}^N=0.3$  mT,  $A_{\perp}^N=0.3$  mT. LINE WIDTH: PARALLEL=0.6 mT, PERPENDICULAR=0.45 mT.  $\nu = 9.052$  GHz

The EPR spectra of the complexes at 77K resulted in a spectrum similar to that of the corresponding metal precursor porphyrin. This observation of EPR lines was due to strong dipolar broadening arising due to interaction between the metal centers. However, the variation in  $g$  and  $A$  values from metal precursors were interpreted using simulation and found two  $g$  values corresponding to two different copper environments and the values were tabulated in **Table 2**.

The degree of distortion from square planar copper complexes and deviation from perfect geometry depending on the coordinated ligand was observed by the ratio  $f = g_{\parallel} / A_{\parallel}$ <sup>22, 23</sup>. In general, the EPR spectra can help in identifying the geometry a complex adopted by using the isotropic parameters  $A_{iso} = (A_{\parallel} + A_{\perp})/3$  and  $g_{iso} = (g_{\parallel} + g_{\perp})/3$ . The values for planar symmetry are between  $A_{iso} = 75-90$  cm<sup>-1</sup> and  $g_{iso} = 2.06 - 2.11$ <sup>24, 25</sup>. From the result it was concluded that each metal centers were close to planar geometry.



No increase in the tetrahedral distortion of the porphyrin ring was observed because of ring stiffness. Also the isomeric values were consistent with a square planar geometry.

**CONCLUSION:** The availability of replaceable proton in *meso*-5-(4-hydroxyphenyl) - 10, 15, 20-tris (4-methylphenyl) porphyrin allows the preparation of new *meso*-monocopperated porphyrin monomers. The electronic spectra show red shift and intensity variation due to perturbation at the *meso*- sites. Electronic ground state interactions are negligible. The peripheral copper Schiff's base complex adapts more planar geometry in the *meso* substituted porphyrin systems than in their pure form. Due to weak interactions between the *meso*-copper ion and central metal ion EPR signals do not show much significant change in the spectrum. The difficulty in undergoing reduction and oxidation of peripheral copper ions and the easiness to undergo reduction and oxidation in the porphyrin ring rationalize that the peripheral copper reaches more planar geometry and the porphyrin structure distorts on complexation.

**ACKNOWLEDGMENT:** ST thanks UGC for fellowship. RV thanks AICTE for financial assistance. Authors thank CDRI, Lucknow, India for providing mass and elemental analysis, SIF, IISc., Bangalore, India for nuclear magnetic resonance, DST FIST and UGC SAP and Dr. J. Subramanian for helpful discussions during EPR analysis.

**CONFLICT OF INTEREST:** No conflict of interest.

## REFERENCES:

1. Virginia Gómez-Vidales, Andres Borja-Miranda, Sandra Cortez-Maya, Oscar Amelines-Sarria, Margarita Rivera and Marcos Martínez-García: Design and Synthesis of a Multi Cu(II)-porphyrin Array. *Open Chemistry Journal*, 2016; 3:
2. Minbo Lan, Hongli Zhao, Huihui Yuan, Chengrui Jiang, Shaohua Zuo, Ying Jiang: Absorption and EPR spectra of some porphyrins and metalloporphyrins. *Dyes and Pigments* 2007; 74: 357-362.
3. Vicente M da GH, Smith KM: Syntheses and Functionalizations of Porphyrin Macrocycles. *Current organic synthesis* 2014; 11(1): 3-28.
4. Taira Imamura, Keiko Fukushima: Self-assembly of metallopyridylporphyrin oligomers. *Coord. chem. rev.*, 2000; 198: 133.
5. Jacek Wojaczynski, Lechoslaw Latos-Grazynski: Poly- and oligometalloporphyrins associated through coordination. *Coord. Chem. Rev.*, 2000; 204: 113
6. Fujita N, Biradha K, Fujita M, Sakamoto S and Yamaguchi K: A porphyrin prism: Structural switching triggered by guest inclusion. *Angew. Chem. Int. Ed. Engl.*, 2001; 40: 1718.
7. Richeter S, Jeandon C, Gisselbrecht J -P, Ruppert R and Callot H J: Synthesis and optical and electrochemical properties of porphyrin dimers linked by metal ions. *J. Am. Chem. Soc.*, 2002; 124: 6168.
8. Burrell A K, Officer D L, Plieger P G and Reid D C W: Synthetic routes to multi-porphyrin arrays. *Chem. Rev.*, 2001; 101: 2751.
9. Yoshikazu Matsushima, Setsuro Sugata, Yako Saionji and Minoru Tsutsui: Meso-tetra [5-(8-hydroxyquinoly)] porphine. A novel porphyrin with metal-chelating groups in the peripheral region. *Chem. Pharm. Bull.* 1980; 28: 2672.
10. Rea N, Loock B and Lexa D: Porphyrins bound to Ru(bpy)<sub>2</sub> clusters: electrocatalysis of sulfite. *Inorg. Chimica Acta*, 2001; 312: 53.
11. Perrin DD and Armarego W L F: Purification of laboratory chemicals, Edition 3, A. Wheaton and Co Ltd., Great Britain, chapter 3, 1988.
12. Adler A D, Longo F R, Finarelli J D, Goldmacher J, Assour J and Korsapoff L: Synthesis of tetraphenylporphin. *J. Org. chem.* 1967; 32: 476.
13. Alan Cowley H: 5,10,15,20-tetrakis(2,6-dihydroxyphenyl)-21H,23H-porphine. *Inorganic synthesis*, John Wiley and sons, New York, 31:1997: 117.
14. Fuhrhop J H and Smith K M: Laboratory methods in porphyrin and metallo-porphyrins research. Elsevier, Amsterdam. 1975.
15. Bencini A, Benelli C, Caneshi A, Carlin R L, Dei A, and Gatteschi D: Crystal and molecular structure of and magnetic coupling in two complexes containing gadolinium (III) and copper(II) ions. *J. Am. Chem. Soc.* 1985; 107: 8128.
16. Fuhrhop J H: The oxidation states and reversible redox reactions of metalloporphyrin. *Struct. Bonding*, 8: 1974: 1.
17. Kadish K M: The electrochemistry of metalloporphyrins in nonaqueous media. *Prog. Inorg. Chem.* 1986; 34: 435.
18. Butler J N: Electrochemistry in dimethyl sulfoxide. *J. Electroanal. Chem.* 1967; 14: 89.
19. Gary Miessler L, Donald Tarr A: *Inorganic Chemistry*. Edition 2, Prentice-Hall International (UK) Ltd., 1999.
20. Sir Geoffrey Wilkinson, Robert Gillard D and Jon McCleverty A: *Comprehensive coordination chemistry*. Wheaton A and Co. Ltd., Great Britain, 1987; 5: 667.
21. Subramanian J: *Porphyrins and Metallo porphyrins*, Smith K M 1975 Ed., Elsevier, Amsterdam, chapter 13.
22. Labanova M, Bidzinska E, Para A: EPR investigation of Cu(II)-complexes with nitrogen derivatives of dialdehyde starch. *Carbohydr. Polym.*, 2012; 87: 2605-2613. [<http://dx.doi.org/10.1016/j.carbpol.2011.11.034>]
23. Pogni R., Baratto M.C., Diaz A., Basosi R.J: EPR characterization of mono (thiosemi-carbazones) copper(II) complexes, note II. *Inorg. Biochemistry*, 2000; 79: 333-339. [[http://dx.doi.org/10.1016/S0162-0134\(99\)00166-X](http://dx.doi.org/10.1016/S0162-0134(99)00166-X)]
24. Suresh E., Bhadbhade M.M., Srinivas D: Molecular association, chelate conformation and reactivity correlations in substituted ophenylenebis (salicylidenato) copper (II) complexes: UV-visible, EPR and X-ray structural investigations. *Polyhedron*, 1996; 15: 4133-4144. [[http://dx.doi.org/10.1016/0277-5387\(96\)00178-7](http://dx.doi.org/10.1016/0277-5387(96)00178-7)]

25. Yu. E. Kandrashkin, V.S. Iyudin, V.K. Voronkova, E.A. Mikhailitsyna, V.S. Tyurin; Continuous-Wave and Time-Resolved Electron Paramagnetic Resonance Study of

Dimerized Aza-Crown Copper Porphyrins Appl Magn Reson 2013; 44: 967–981.

**How to cite this article:**

Tamijselvy S and Venkatesan R: Design and synthesis of bi-metallic porphyrin array. Int J Pharm Sci Res 2017; 8(8): 3361-70.doi: 10.13040/IJPSR.0975-8232.8(8).3361-70.

All © 2013 are reserved by International Journal of Pharmaceutical Sciences and Research. This Journal licensed under a Creative Commons Attribution-NonCommercial-ShareAlike 3.0 Unported License.

This article can be downloaded to **ANDROID OS** based mobile. Scan QR Code using Code/Bar Scanner from your mobile. (Scanners are available on Google Playstore)